

# The CALSPEC Stars P177D and P330E

Ralph C. Bohlin<sup>1</sup> and Arlo U. Landolt<sup>2</sup>

bohlin@stsci.edu

landolt@phys.lsu.edu

## ABSTRACT

Multicolor photometric data are presented for the CALSPEC stars P177D and P330E. Together with previously published photometry for nine other CALSPEC standards, the photometric observations and synthetic photometry from HST/STIS spectrophotometry agree in the B, V, R, and I bands to better than  $\sim 1\%$  (10 mmag).

*Subject headings:* stars:individual — stars:fundamental parameters (absolute flux) — techniques:photometry

## 1. INTRODUCTION

The CALSPEC<sup>1</sup> stars are a group of spectrophotometric flux standards used to calibrate instrumentation on the Hubble Space Telescope (HST) Bohlin (2007), Bohlin et al. (2014, B14). P177D is of spectral type G0 V and P330E is of spectral type G2 V. Originally, Colina & Bohlin (1997) quoted G0 V for P330E, while the revision to G2 V from Simbad is reasonable, based on the similarity to the Solar spectral energy distribution (SED) as illustrated in figure 8 of B14. The J2000 coordinates from SIMBAD are listed in Table 1. Most of the additional CALSPEC stars are presented in Landolt & Uomoto (2007b,a), while GD71 appears in Landolt (1992, 2009). The previously unpublished GD153 is included in Table 1 with its rms scatter, because the error-in-the-mean is not valid with only four measures. The two G stars, P177D and P330E, are crucial additions for cross-comparison of the Landolt and CALSPEC data, because most of the other stars in common are of much hotter spectral types.

The photometric observations are described in Section 2, while Section 3 discusses the comparison of the actual Landolt photometry with the synthetic CALSPEC photometry.

---

<sup>1</sup>Space Telescope Science Institute, 3700 San Martin Drive, Baltimore, MD 21218, USA

<sup>2</sup>Department of Physics and Astronomy Louisiana State University Baton Rouge, Louisiana 70803

<sup>1</sup><http://www.stsci.edu/hst/observatory/crds/calspec.html>

## 2. OBSERVATIONS

The broad-band UBVR photometric data for P177D and P330E were obtained during two observing runs, separated by one year, at the Lowell Observatory’s 1.8-m Lowell Perkins telescope. A complete data set for an observation of a star consisted of a series of measures VBURIIRUBV. The data acquisition, reduction and analysis have been described in Landolt (2013) and also see Landolt (2007). The new photometry for P177D and P330E is tied to the standard stars of Landolt (2009). Final magnitudes and color indices for P177D and P330E are given in Table 1. The uncertainty (Unc) beneath each magnitude or color index is the rms mean error for a single observation.

The individual data points that were used to derive the final magnitudes and color indices are shown in Table 2. The UT date of observation is given in the second column, followed by the Heliocentric Julian Date (HJD) of the central time of each observation. The remaining columns list the magnitude and color indices from each observation. Each star was measured twice a night on five nights over a one year time interval, i.e. ten measures total for each star. Immediately beneath the final magnitude and color indices are two lines indicating the averages and rms  $1\sigma$  errors for a single observation of each magnitude or color index. The final line provides the mean error of the mean, i.e. the uncertainty in the mean, for the star’s magnitude or color index.

Perhaps, the largest source of error in ground-based photometry is from the air mass extinction, which is described in Landolt (2007). In summary, the air mass correction is derived from 4–6 stars in standard fields that are observed every few hours on every night at air-mass values similar to the program stars. The extinction for any program star is interpolated in time from the set of standard star determinations. Small air mass differences between standards and program stars are accounted by differences in the secant of the zenith angles. Rapid changes in atmospheric transmission will cause errors of order 0.01 mag, but the expectation is that those errors are random and will be reduced by repeated observations of the program stars over many nights. Because the atmospheric extinction decreases with wavelength from U to I (Hayes & Latham 1975), better agreement between space and ground based fluxes might be expected in the longer wavelength filters, except that there are strong time-variable absorption lines due to H<sub>2</sub>O in the I band. Thus, our focus is on V and R for the Landolt/CALSPEC comparison.

### 2.1. Variability of BD+17°4708

Figure 1 shows the individual observations of the Sloan standard BD+17°4708 (Fukugita et al. 1996), which are the basis for the magnitude and color indices of BD+17°4708 in table 4 of Landolt & Uomoto (2007b). Linear fits to the data points after JD2446500 in 1986 suggest that star is variable with an increase in flux of  $\sim 8$  mmag/yr in bands UBVR over the 1986–91 time period. The statistical significance of this brightening ranges up to  $7\sigma$ , while similar analyses for other program stars produce slopes with less than  $\sim 3\sigma$  significance. The second most likely variable is GRW+70°5824 with a decline in brightness in U and B of 5–6 mmag/yr, but with only

$3\sigma$  significance; in VRI, the decline is  $\sim 3$  mmag/yr with only  $2\sigma$  significance.

### 3. DISCUSSION

#### 3.1. Equations

The HST CALSPEC standard star spectrophotometry  $F_\lambda$  with units  $\text{erg cm}^{-2} \text{ s}^{-1} \text{ \AA}^{-1}$  is compared with Landolt photometry using the technique of synthetic photometry. The mean flux in wavelength units over a photometric bandpass function  $R$  is

$$\langle F \rangle = \frac{\int F_\lambda \lambda R d\lambda}{\int \lambda R d\lambda} \quad (1)$$

(Bohlin et al. 2014; Bessell & Murphy 2012), where  $R$  is the unitless system transmission or quantum efficiency (QE). A particular magnitude system is defined relative to a reference flux  $\langle F_o \rangle$  as,

$$m_\lambda = -2.5 \log(\langle F \rangle / \langle F_o \rangle) = -2.5 \log(\langle F \rangle) + ZP, \quad (2)$$

e.g. for Vega magnitudes, which are defined as zero at all wavelengths; and  $\langle F \rangle = \langle F_o \rangle$  would be the CALSPEC flux of Vega (*alpha\_lyr\_stis.008.fits*). However, the Johnson magnitudes of Vega are non-zero; and the Johnson zero point (ZP) for each star is

$$ZP = 2.5 \log(\langle F_o \rangle) = m_\lambda + 2.5 \log(\langle F \rangle), \quad (3)$$

where  $m_\lambda$  is the Landolt stellar magnitude on the Johnson system and  $\langle F \rangle$  is the Equation (1) integral of the CALSPEC fluxes.

#### 3.2. Comparison of Landolt Photometry with CALSPEC SEDs

For the comparison of the Landolt UBVRI photometry with the CALSPEC SEDs, bandpass functions from Cohen et al. (2003), Maíz Apellániz (2006), and Bessell & Murphy (2012) are investigated. Bessell & Murphy (2012) say that smooth functions must be fit to their coarsely sampled bandpasses; but fitting splines sampled every Angstrom makes less than 0.001 mag difference in the computed synthetic photometry. While Maíz Apellániz (2006) and Bessell & Murphy (2012) estimate the actual Johnson-Cousins system throughput for the filters, the Cohen functions are from measured transmission of the Landolt filters as multiplied by typical atmospheric transmission. Because the Cohen bandpass functions are based on measurements and are estimates for the actual Landolt instrumentation, the color transformations from the instrumental magnitudes to the Johnson-Cousins system must be added to the synthetic photometry. Also, the Cohen bandpasses differ from Maíz Apellániz and Bessell and from the QE  $R$  in Equation (1), i.e. there is a wavelength factor  $\lambda$  included. Thus, the Cohen bandpass functions must be divided by  $\lambda$  for comparison

with Maíz Apellániz and Bessell. The wavelength vectors for all three ground-based systems are converted to vacuum before multiplication by the CALSPEC vacuum SEDs  $F_\lambda$  in Equation (1).

For each band in each system, the ZPs from Equation (3) are computed for each star; and the weighted mean and rms of the zero points are compiled in Table 3, where the best agreement is for the Maíz Apellániz V with only 0.007 mag of scatter among the 11 non-variable stars. For example, Figure 2 illustrates the differences between Landolt and CALSPEC for this best case, where BD+17°4708 is shown but not included in the rms scatter. However, the two coolest stars, P177D and P330E, are high in comparison with the hot stars. This systematic trend could be ameliorated if the bandpass function is slightly in error.

Figure 3 illustrates the three V bandpasses in comparison with the steep SED for a hot star and a flatter SED for a cooler star. A shift of any bandpass toward shorter wavelengths decreases the relative synthetic flux ratio of the cool to hot star. While the Bessell bandpass produces similar results to the Maíz Apellániz results in Figure 3, the Cohen results are in the opposite sense, where a shift of the Cohen bandpass toward longer wavelengths would be required to improve the cool/hot star agreement. Only Cohen and Bessell provide bandpass functions for all of the five Landolt bands; and Table 3 shows that the Cohen rms is generally the worst, despite his valient attempt to derive the transmissions directly from first principles. Thus, for a uniform result across all five bands, the Bessell bands are slightly shifted in order to minimize the rms scatter for the 11 stars. These wavelength shifts for optimizing the Landolt/CALSPEC comparison are in Table 4 along with the optimum zero-point reference fluxes  $F_o$ , the zero points in mag, and rms scatter, while Figure 4 illustrates the improvement over Figure 2 for the V band. There are only 12 CALSPEC stars with Landolt photometry and complete STIS coverage of the V band. However, there are an additional four stars with complete coverage in R and I. Figure 5 also shows sub-percent agreement between the actual and synthetic photometry in the shifted Bessell R band, where the atmospheric extinction and time-variable absorption lines are minimal and comparable to the V band. In V, only AGK+81° 266 shows as much as a  $2\sigma$  difference between the actual and synthetic CALSPEC photometry; and similarly in R, there are no serious discrepancies from perfect agreement between the two independent measures of stellar flux, (except for the variable star BD+17°4708, which differs by 0.014 mag in both V and R).

While the Bessell bandpasses are referenced to photometry with considerable weight on SAAO data, Menzies et al. (1991) found small systematic differences between SAAO and Landolt photometry as a function of RA. Our shifts of the Bessell bands may represent actual differences between SAAO and Landolt bandpasses or, perhaps, just reflect subtle differences between the SAAO and Landolt representations of the UBVRI system.

Using the optimally shifted Bessell bandpasses for the 11 or 15 non-variable stars, Table 5 contains the magnitudes and uncertainties of Vega on the Johnson-Cousins system of UBVRI photometry, where  $m(Vega)$  is defined by Equation (2) using the version *stis\_008* CALSPEC flux  $F(Vega)$ . The uncertainties are just for the conversion to magnitudes and do not include any

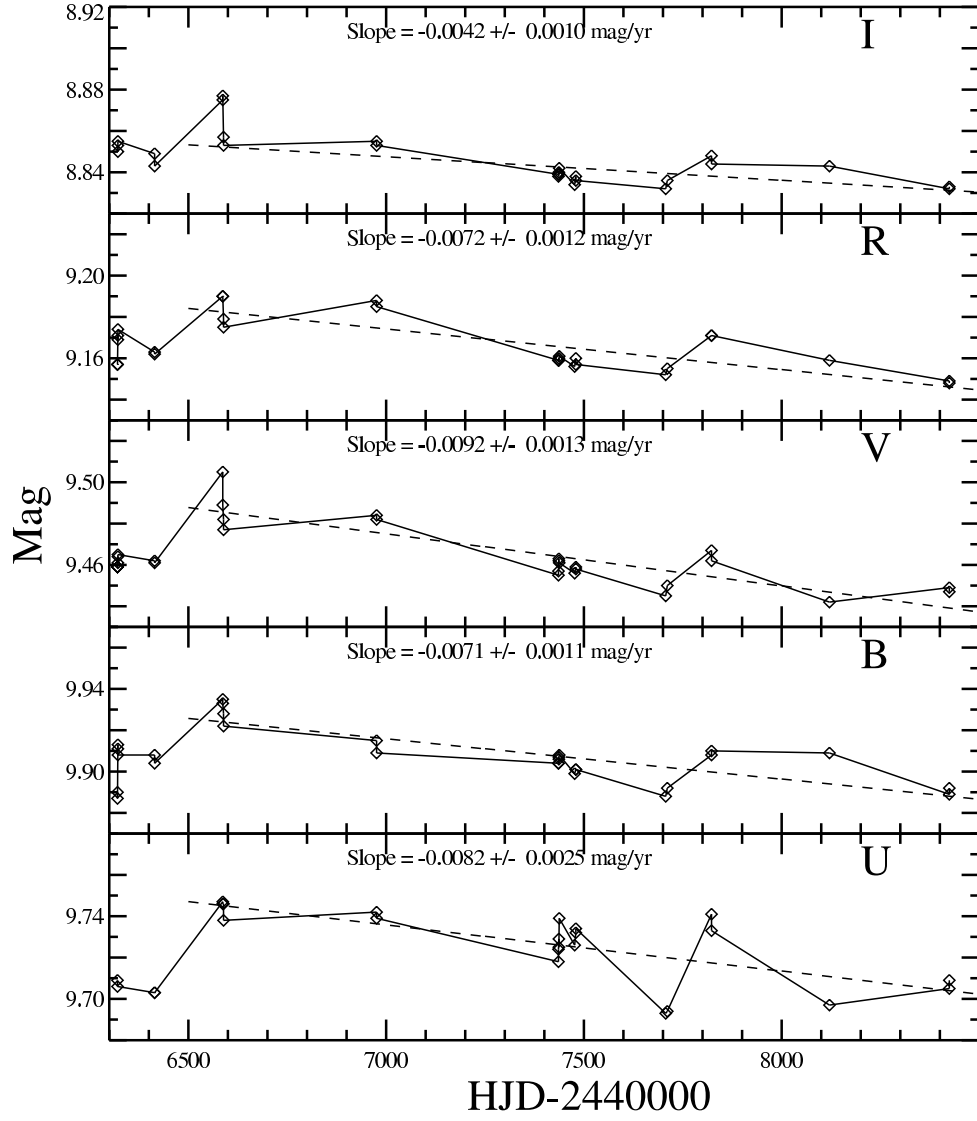
uncertainty in the CALSPEC flux itself. For comparison, Table 5 also includes UBVRI from Bessell & Murphy (2012) and the original measures of Johnson et al. (1966). Our results agree well with Bessell & Murphy (2012), except in the problematic U band where variable atmospheric extinction provides the short wavelength cutoff of the filter transmission function. The Johnson et al. (1966) photometry also agrees within 0.01 mag in B and V but should not be expected to agree for the more commonly used Cousins R and I bandpasses used here.

As a final check for systematic errors, Figure 6 shows the same optimized difference in photometry vs. air mass for the V band. The weighted linear, least square fit suggests that any systematic error in the airmass correction is less than 5 mmag. The slope of the fitted line differs from zero by less than  $3\sigma$ , so that our data are consistent with no error in the airmass correction.

AUL wishes to thank the then Diretor of Lowell Observatory, Robert L. Millis, for generous telescope time assignments for his photometric standard star program. This aspect of AUL’s observational program has been supported by NSF grants AST-0503871 and AST 0803158. Primary support for RCB was provided by NASA through the Space Telescope Science Institute, which is operated by AURA, Inc., under NASA contract NAS5-26555. This research made use of the SIMBAD database, operated at CDS, Strasbourg, France.

Table 1. Average UBVRI Photometry and rms Uncertainty for P177-D and P330-E

Star	RA (2000)	DEC (2000)	V	B-V	U-B	V-R	R-I	V-I
P177-D	15 59 13.579	+47 36 41.91	13.492	+0.646	+0.156	+0.364	+0.371	+0.737
Unc in Mean			0.004	0.009	0.016	0.004	0.010	0.013
P330-E	16 31 33.82	+30 08 46.5	13.028	+0.630	+0.070	+0.362	+0.362	+0.726
Unc in Mean			0.004	0.006	0.010	0.007	0.007	0.008
GD153	12 57 02.337	+22 01 52.68	13.349	-0.289	-1.177	-0.139	-0.180	-0.320
rms			0.008	0.007	0.010	0.013	0.017	0.005



Bohlin: ptarlo 31-Oct-2014 16:48

Fig. 1.— Variation of the brightness of BD+17°4708 in various bands.

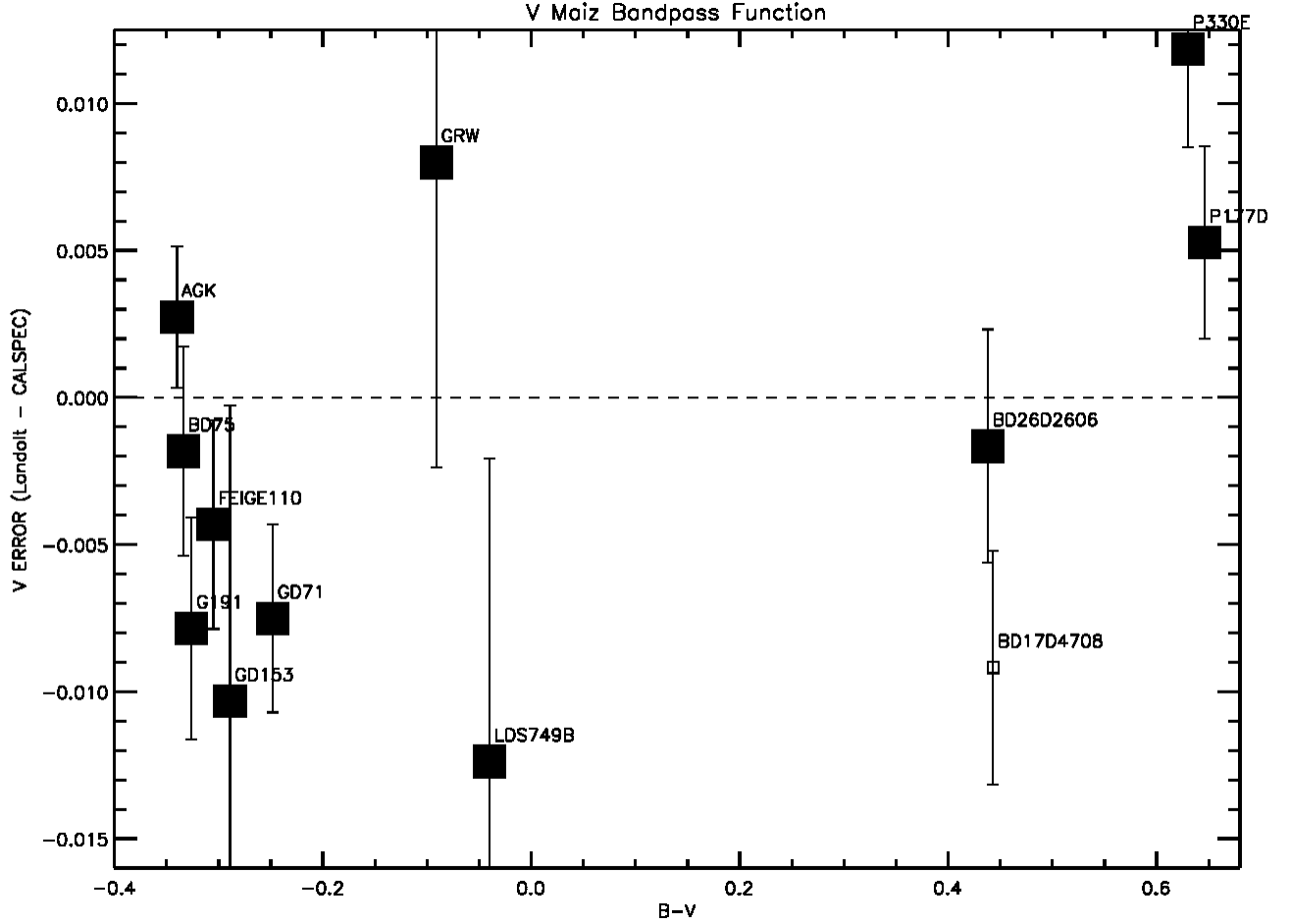


Fig. 2.— Comparison of STIS synthetic photometry to Landolt actual photometry in the V band using the Maíz Apellániz (2006) bandpass function for the synthetic photometry. The poorly observed GRW+70°5824 and the faint LDS749B have large STIS uncertainties. GD153 was observed only four times by Landolt.

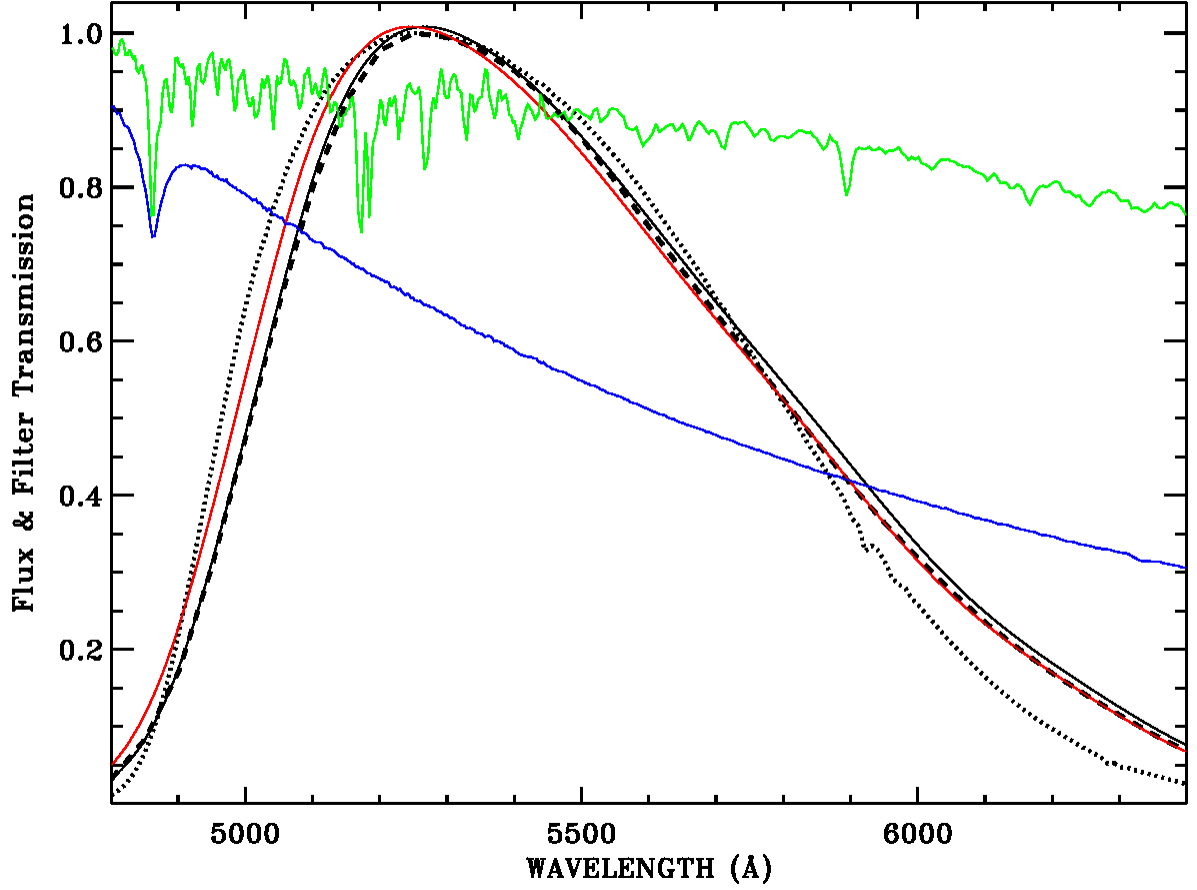


Fig. 3.— Normalized V band filter curves from Cohen et al. (2003):dots, Maíz Apellániz (2006):dash, and Bessell & Murphy (2012):solid. The Cohen relative response has been divided by wavelength. Normalized CALSPEC SEDs are shown for G191B2B:blue and for P330E:green. The red curve is the Bessell bandpass shifted by  $-20 \text{ \AA}$  to minimize the Landolt/CALSPEC differences.



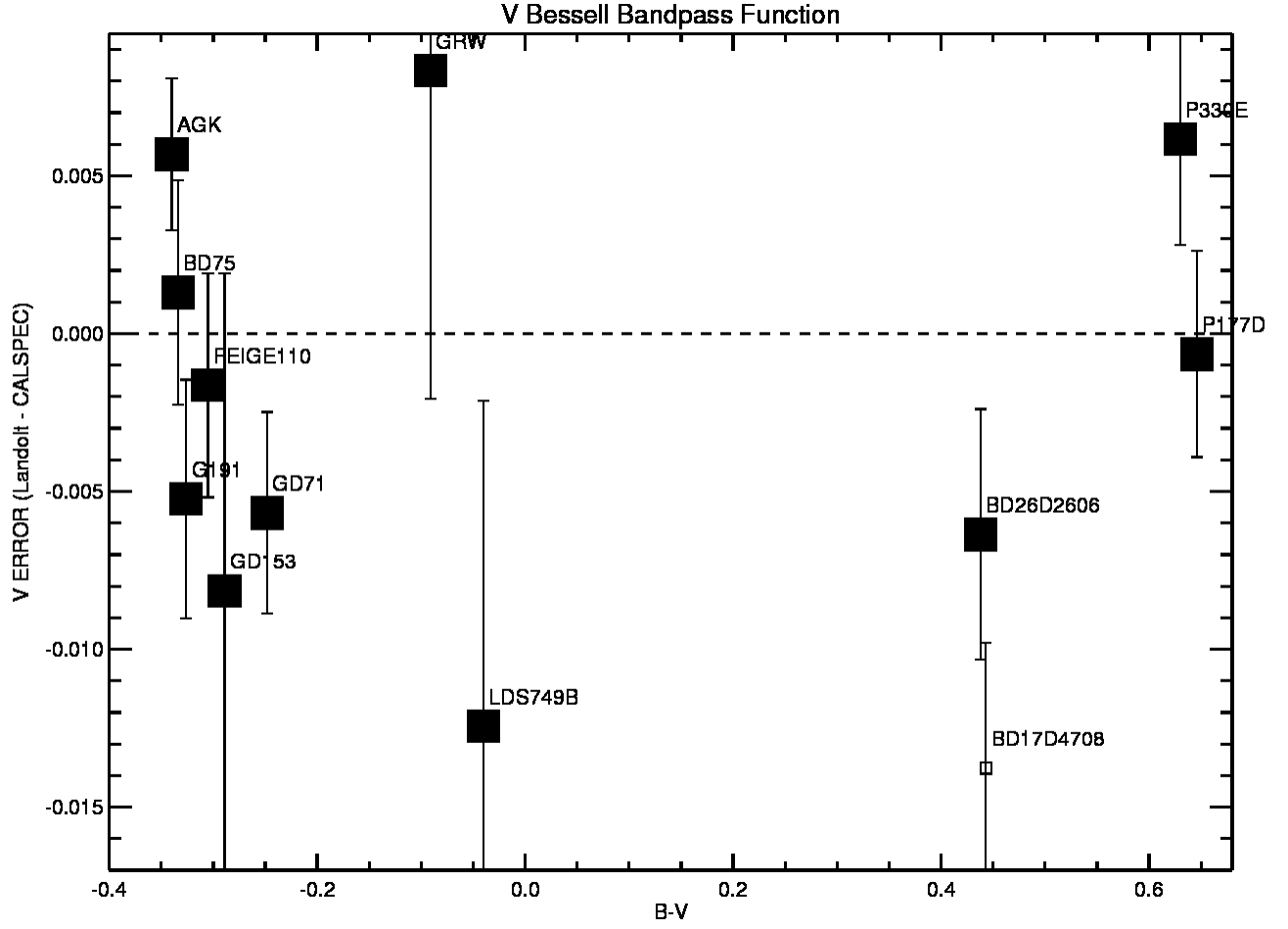


Fig. 4.— As in Figure 2 except for the Bessell & Murphy (2012) bandpass shifted by  $-20 \text{ \AA}$  to optimize the agreement of the actual and synthetic photometry.

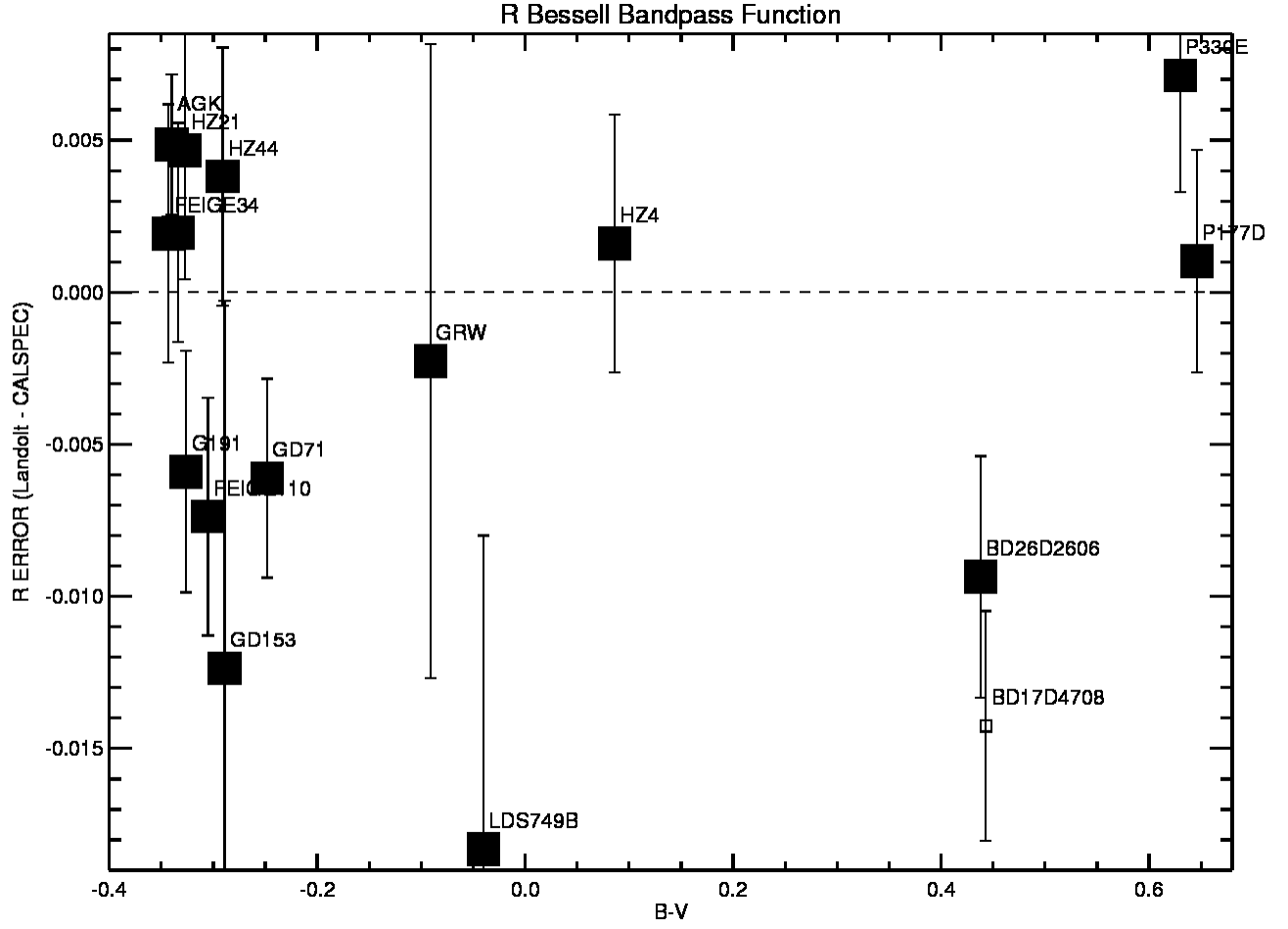


Fig. 5.— As in Figure 4 except for the R band shifted by  $-31 \text{ \AA}$  to optimize the agreement of the actual and synthetic photometry.

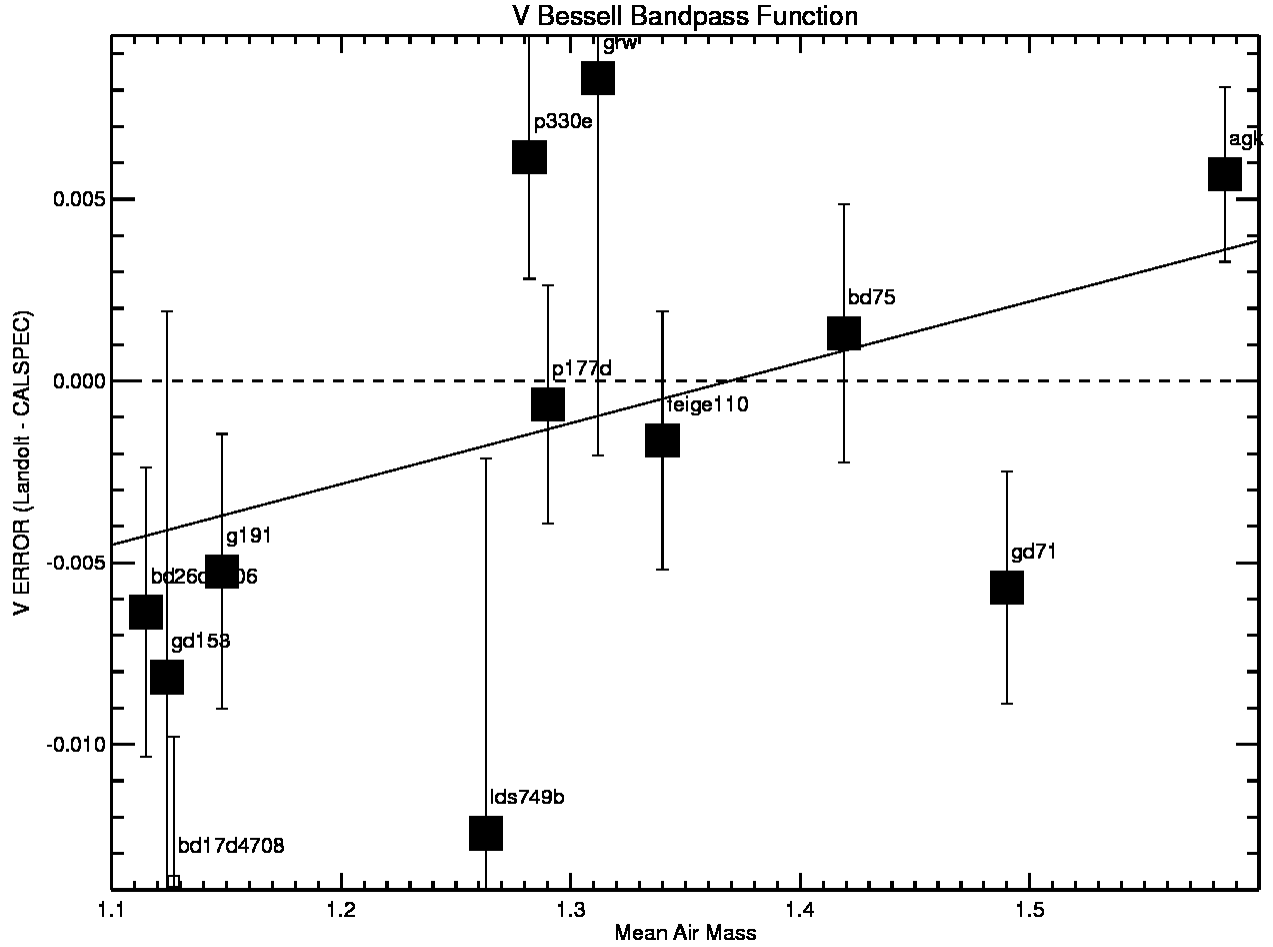


Fig. 6.— As in Figure 2, except plotted vs. air mass and for the shifted Bessell & Murphy (2012) bandpass function. The solid line is the weighted linear, least-square fit to the 11 filled black squares.

Table 2. Individual Observations

Star	UT Date mmddyy	HJD	V	B-V	U-B	V-R	R-I	V-I
P177-D	080907	2454321.70656	13.489	+0.638	+0.155	+0.363	+0.373	+0.738
P177-D	080907	2454321.71088	13.492	+0.645	+0.162	+0.367	+0.371	+0.741
P177-D	081007	2454322.71172	13.497	+0.667	+0.124	+0.362	+0.363	+0.728
P177-D	081007	2454322.71626	13.500	+0.634	+0.169	+0.358	+0.361	+0.722
P177-D	081107	2454323.71285	13.486	+0.637	+0.172	+0.357	+0.356	+0.715
P177-D	081107	2454323.71722	13.489	+0.649	+0.157	+0.358	+0.368	+0.729
P177-D	090308	2454712.68389	13.495	+0.652	+0.161	+0.367	+0.394	+0.763
P177-D	090308	2454712.68863	13.491	+0.641	+0.177	+0.367	+0.374	+0.744
P177-D	090408	2454713.66759	13.490	+0.652	+0.143	+0.369	+0.376	+0.746
P177-D	090408	2454713.67186	13.490	+0.650	+0.139	+0.369	+0.370	+0.740
Avg			13.492	+0.646	+0.156	+0.364	+0.371	+0.737
rms			0.004	0.009	0.016	0.004	0.010	0.013
Unc in Mean		n = 10	0.0013	0.0028	0.0051	0.0013	0.0032	0.0041
P330-E	080907	2454321.71661	13.036	+0.622	+0.066	+0.370	+0.348	+0.721
P330-E	080907	2454321.72013	13.025	+0.624	+0.071	+0.364	+0.360	+0.726
P330-E	081007	2454322.72194	13.030	+0.634	+0.075	+0.352	+0.371	+0.725
P330-E	081007	2454322.72544	13.031	+0.633	+0.077	+0.354	+0.358	+0.715
P330-E	081107	2454323.72212	13.023	+0.623	+0.077	+0.365	+0.356	+0.724
P330-E	081107	2454323.72562	13.028	+0.622	+0.070	+0.362	+0.371	+0.735
P330-E	090308	2454712.69367	13.024	+0.639	+0.078	+0.354	+0.363	+0.720
P330-E	090308	2454712.69747	13.030	+0.638	+0.076	+0.362	+0.356	+0.720
P330-E	090408	2454713.67720	13.021	+0.635	+0.054	+0.365	+0.369	+0.736
P330-E	090408	2454713.68053	13.032	+0.629	+0.050	+0.373	+0.366	+0.740
Avg			13.028	+0.630	+0.070	+0.362	+0.362	+0.726
rms			0.004	0.006	0.010	0.007	0.007	0.008
Unc in Mean		n = 10	0.0013	0.0019	0.0032	0.0022	0.0022	0.0025

Table 3. Average Zero Points and rms Scatter for Three Bandpass Functions

Ref.	ZP or rms	U	B	V	R	I
Cohen et al. (2003)	ZP <sup>a</sup>	4.483	6.831	3.772	2.263	1.121
	ZP	-20.871	-20.414	-21.059	-21.614	-22.376
	rms	0.065	0.040	0.011	0.008	0.018
Maíz Apellániz (2006)	ZP <sup>a</sup>	4.238	6.333	3.674		
	ZP	-20.932	-20.496	-21.087		
	rms	0.015	0.011	0.007		
Bessell & Murphy (2012)	ZP <sup>a</sup>	4.212	6.314	3.659	2.198	1.169
	ZP	-20.939	-20.499	-21.092	-21.645	-22.330
	rms	0.017	0.013	0.008	0.008	0.010

<sup>a</sup> $\langle F_o \rangle$  ( $10^{-9}$  erg cm $^{-2}$  s $^{-1}$  Å $^{-1}$ ). Other ZP and rms values are mag units.

Table 4. Shifts, ZPs, and rms Scatter for the Optimized Bessell Bandpass Functions

Band	Shift (Å)	ZP= $\langle F_o \rangle$ ( $10^{-9}$ erg cm $^{-2}$ s $^{-1}$ Å $^{-1}$ )	ZP (mag)	rms (mag)
U	-8	4.232	-20.934	.0160
B	-20	6.396	-20.485	.0073
V	-20	3.700	-21.079	.0054
R	-31	2.236	-21.626	.0059
I	-27	1.184	-22.317	.0096

Table 5. Magnitudes and Uncertainty for Vega using the Shifted Bessell Bandpass Functions

Star	RA (2000)	DEC (2000)	U	B	V	R	I
Vega	18 36 56.336	+38 47 01.28	0.064	0.020	0.028	0.033	0.029
rms			0.016	0.007	0.005	0.006	0.010
Unc in Mean			0.007	0.004	0.003	0.003	0.004
Bessell			0.041	0.023	0.027	0.027	0.028
Johnson			0.03	0.03	0.03	0.07 <sup>a</sup>	0.10 <sup>a</sup>

<sup>a</sup>These Johnson R and I values are not expected to agree with the shorter wavelength Cousins R and I values in the rest of the Table.

## REFERENCES

- Bessell, M., & Murphy, S. 2012, *PASP*, 124, 140
- Bohlin, R. C. 2007, in *Astronomical Society of the Pacific Conference Series*, Vol. 364, *The Future of Photometric, Spectrophotometric and Polarimetric Standardization*, ed. C. Sterken, 315
- Bohlin, R. C., Gordon, K. D., & Tremblay, P.-E. 2014, *PASP*, 126, 711 (B14)
- Cohen, M., Megeath, S. T., Hammersley, P. L., Martín-Luis, F., & Stauffer, J. 2003, *AJ*, 125, 2645
- Colina, L., & Bohlin, R. 1997, *AJ*, 113, 1138
- Fukugita, M., Ichikawa, T., Gunn, J. E., et al. 1996, *AJ*, 111, 1748
- Hayes, D. S., & Latham, D. W. 1975, *ApJ*, 197, 593
- Johnson, H. L., Mitchell, R. I., Iriarte, B., & Wisniewski, W. Z. 1966, *Communications of the Lunar and Planetary Laboratory*, 4, 99
- Landolt, A. U. 1992, *AJ*, 104, 340
- Landolt, A. U. 2007, in *Astronomical Society of the Pacific Conference Series*, Vol. 364, *The Future of Photometric, Spectrophotometric and Polarimetric Standardization*, ed. C. Sterken, 27
- . 2009, *AJ*, 137, 4186
- . 2013, *AJ*, 146, 131
- Landolt, A. U., & Uomoto, A. K. 2007a, *AJ*, 133, 2429
- . 2007b, *AJ*, 133, 768
- Maíz Apellániz, J. 2006, *AJ*, 131, 1184
- Menzies, J. W., Marang, F., Laing, J. D., Coulson, I. M., & Engelbrecht, C. A. 1991, *MNRAS*, 248, 642